Published in final edited form as:
Org Biomol Chem. 2009 October 7; 7(19): 3969–3975. doi:10.1039/b907664f.

Fluorogenic affinity label for the facile, rapid imaging of proteins in live cells

Rex W. Watkins[a], **Luke D. Lavis**[†,b], **Vanessa M. Kung**[b], **Georgyi V. Los**[c], and **Ronald T. Raines**[a,b,*]

[a]Department of Biochemistry, University of Wisconsin–Madison, 433 Babcock Drive, Madison, WI 53706, USA

[b]Department of Chemistry, University of Wisconsin–Madison, 1101 University Avenue, Madison, WI 53706, USA

[c]Promega Corporation, 2800 Woods Hollow Road, Madison, WI 53711, USA

Abstract

Haloalkane dehalogenase (HD) catalyzes the hydrolysis of haloalkanes via a covalent enzyme–substrate intermediate. Fusing a target protein to an HD variant that cannot hydrolyze the intermediate enables labeling of the target protein with a haloalkane *in cellulo*. The utility of extant probes is hampered, however, by background fluorescence as well as limited membrane permeability. Here, we report on the synthesis and use of a fluorogenic affinity label that, after unmasking by an intracellular esterase, labels an HD variant *in cellulo*. Labeling is rapid and specific, as expected from the reliance upon enzymic catalysts and the high membrane permeance of the probe both before and after unmasking. Most notably, even high concentrations of the fluorogenic affinity label cause minimal background fluorescence without a need to wash the cells. We envision that such fluorogenic affinity labels, which enlist catalysis by two cellular enzymes, will find utility in pulse–chase experiments, high-content screening, and numerous other protocols.

Introduction

The labeling of proteins with genetically encoded autofluorescent proteins has revolutionized cell imaging.[1] These “tags” can reveal subcellular localization, dynamics, and chemical environment.[2] Nonetheless, the utility of autofluorescent proteins has notable limitations, including the restriction of “one clone–one color” and an inability to label temporally disparate pools of protein by using a single genetic construct, thereby precluding pulse–chase as well as other types of experiments.

A recent development has overcome some limitations of autofluorescent proteins. Specifically, genetically encoded enzymic tags now enable the use of small-molecule fluorophores to label proteins *in cellulo*.[3–6] A key advantage of these systems is their modularity. With a single genetic construct, a wide variety of substrate analogs, including fluorophores with disparate spectral properties,[3] can be attached to a fusion protein of interest (*i.e.*, one clone–many colors) at any time. In addition, this approach avails the high reactivity that has evolved within enzymic active sites. Second-order rate constants for enzyme-mediated labeling have been reported to

*To whom correspondence should be addressed: rtraines@wisc.edu.
†Current address: Janelia Farm Research Campus, Howard Hughes Medical Institute, 19700 Helix Drive, Ashburn VA 20147, USA

Supporting Information
^{1}H and ^{13}C NMR spectra.

be as high as $2.7 \times 10^6\ M^{-1}s^{-1}$,[4] which exceeds by over a million-fold any rate constant reported for a chemoselective labeling reaction involving only small molecules (such as variations of the Huisgen 1,3-dipolar azide–alkyne cycloaddition or Staudinger ligation).[5–7]

Haloalkane dehalogenase (HD; EC 3.8.1.5) is perhaps the most often-used enzymic fusion tag. This enzyme catalyzes the hydrolysis of haloalkanes via a covalent enzyme–substrate intermediate that undergoes hydrolysis. An HD variant that cannot perform the second, hydrolysis step (HaloTag®) reacts rapidly and specifically to form a covalent adduct with a wide variety of chloroalkanes, including assorted fluorophores of varied spectral and physiochemical properties.[8,4]

Still, problems remain with HD and other enzymic fusion tags. Background fluorescence from excess probe and the inefficient passage of small-molecule probes through cellular membranes are especially problematic, necessitating long incubation times or vigorous washing steps. We reasoned that a latent fluorophore based on the venerable trimethyl lock system[9,10] could both diminish background fluorescence and enhance cellular delivery. Accordingly, we designed and synthesized probe **1** (Figure 1) as an affinity label for HD and tested its ability to label HD in living cells. The results are indicative of an advantageous means to label proteins *in cellulo*.

Results and discussion

Design and synthesis of probe 1

The design of probe **1** was based on previous work in which the trimethyl lock system was used to mask the intrinsic fluorescence or absorbance of a small molecule.[11–19] The trimethyl lock moiety is stable to spontaneous hydrolysis, but susceptible to intracellular esterase-catalyzed hydrolysis. The use of a urea moiety rather than a second trimethyl lock allows for single-hit kinetics and the facile addition of reactive groups for bioconjugation.[12] The trimethyl lock–urea system is modular, accommodating a variety of dyes and appendages for bioconjugation.[11–19]

We synthesized probe **1** by condensing two fragments: a fluorogenic substrate for a cellular esterase and a chloroalkane affinity label for HD (Scheme 1). Briefly, known *t*-Boc–rhodamine **4**[12] was subjected to reaction with an *in situ*-generated isocyanate from protected succinate **5**[20] to generate *t*-Boc–rhodamine–urea **6**. Deprotection with trifluoroacetic acid furnished the urea–rhodamine **7** that underwent carbodiimide-mediated coupling with trimethyl lock acid **8**[21] to give benzyl-protected **9**. Removal of the benzyl group by catalytic hydrogenation at −5 °C[22] afforded acid **10**. Activation of the acid to the succimidyl ester, followed by reaction with alkyl chloride **11** gave the desired probe **1**.

Cell imaging with probe 1

We compared the utility of probe **1** for live-cell imaging with that of known probes **2** (diAcFAM) and **3** (R110Direct™). In these experiments, we used a cell line, U2OS, that had been stably transfected to produce a nucleus-directed HD variant (HaloTag®–NLS_3). The nuclear envelope is covered with pores that allow small molecules such as probes **1**–**3** to enter the nucleus by passive diffusion from the cytosol.[23]

We found that images of U2OS cells exposed to probes **1**–**3** differed significantly. Incubation of cells with probes **2** and **3** resulted in non-specific fluorescence after 15 min (Figure 2A). This unsolicited fluorescence was intracellular for **2** and extracellular for **3**. In contrast, probe **1** showed remarkable specificity with virtually no background fluorescence. Additionally, imaging with **1** was strikingly rapid, as images had developed nearly fully after only 10 min

(Figure 2B). Labeling with a ten-fold higher concentration of **1** retained specificity without a large increase in background fluorescence (Figure 2C).

We suspected that the variation in labeling between the fluorogenic affinity labels **1** and **2** is due to differing abilities of the masked and unmasked probes to cross the cell membrane. Although masked **1** and **2** have a net charge of $Z = 0$, unmasked **1** has $Z = 0$ whereas unmasked **2** has $Z = -2$. Cell images suggest that unmasked **2** that has not reacted with the HD variant becomes trapped in the cell, leading to intracellular background fluorescence (Figure 2A*ii* and *v*). Conversely, unmasked **1** that has not reacted with the HD variant can exude from the cell, leading to low background fluorescence.

The low background fluorescence observed with probe **1** could be attributed solely to the latency of its fluorescence. To address this issue, we treated probes **1** and **2** with porcine liver esterase prior to the no-wash labeling procedure. As anticipated from its net charge of $Z = -2$, unmasked **2** was largely membrane impermeant (Figure 2D*ii*). Remarkably, unmasked **1** (Figure 2D*i*) displayed much less intracellular and extracellular background fluorescence than did **3** (Figure 2D*iii*). These data demonstrate that the fluorescence-masking trimethyl lock moiety is not the singular determinant for preventing extracellular background fluorescence. Rather, the intrinsic cell-permeability of probe **1**, in its masked and unmasked state, plays an important role.

Probe lipophilicity

To seek an explanation for the differences in probe internalization, we first calculated the value of log*D*[24,25] for the predominant form of relevant labels at pH 7.4 (Table 1). Because increased lipophilicity generally correlates with increased membrane permeability,[26] probes with higher log*D* values are expected to permeate the membrane more rapidly. The relatively low calculated log*D* value of unmasked **2** corresponds with its slower rate of internalization. There is, however, only a small difference between the calculated values of unmasked **1** and **3**, even though cell-imaging experiments demonstrate that unmasked **1** is much more membrane permeant (Figure 2D).

The inconsistency in the anticipated and demonstrated membrane permeability led us to hypothesize that the increased rate of internalization of unmasked **1** relative to **3** is due to perturbation of the lactone–quinoid equilibrium of the two rhodamine-based dyes[12] (Figure 3). We reasoned that electron-withdrawal by the urea moiety shifts the equilibrium somewhat from the relatively membrane-impermeant quinoid (which is zwitterionic and hence polar) to the lactone.

To investigate the propensity of rhodamine–urea dyes to form the lactone, we determined the effect of solvent dielectric constant (ε) on the lactone–quinoid equilibrium of unmasked **1** and related compounds **12** (rhodamine 110) and **13** (a rhodamine–urea).[12] The ultraviolet–visible spectrum of the quinoid is characterized by a relative absorbance maximum at ~500 nm, which is absent in the spectrum of the lactone.27 The value of ε was varied by altering dioxane/water ratios.[28] We found that formation of the less polar lactones of unmasked **1** and **13**, which contain a urea moiety, is favorable in solutions of higher polarity than with compound **12** (Figure 4). We conclude that the increased rate of internalization of rhodamine–urea dyes is likely due to their increased propensity for lactone formation. This feature ameliorates the difficulty of cell-membrane penetration and lowers background fluorescence.

Recapitulation

Together, the data indicate that probe **3**, which is always fluorescent, is not especially membrane-permeant and produces much extracellular, background fluorescence with our

rapid-imaging protocol (Figure 2A, panels *iii* and *vi*). Although the acetyl groups of probe **2** mask its fluorescence, these groups are vulnerable to hydrolysis in cell-free medium and even PBS.[12] At short time scales (*i.e.*, minutes), the resultant unmasking is not a severe problem. The intracellular background is due to the anionic unmasked fluor that has not reacted with the HD protein but cannot exit the cell because of its membrane impermeance. Only probe **1** has the attributes necessary.

Conclusions

We have demonstrated that probe **1** is a useful cell-permeant affinity label for the facile, rapid labeling of target proteins in live cells. The omission of wash steps is particularly advantageous for the labeling of proteins in non-adherent cells, which are more tedious to separate from excess probe than are adherent cells. In addition, as probe **1** exhibits low background fluorescence, little effort is needed to determine a useful concentration. This attribute could be useful for the labeling of target proteins within a population of transiently transfected cells. The rapidity of cellular labeling with probe **1** enables interrogations with high temporal resolution. This attribute is particularly beneficial for pulse–chase experiments, which require differential labeling of temporally disparate pools of protein. Finally, we suspect that probe **1** will be useful in high-content screens, wherein wash steps, optimization of label concentration, and probe instability are especially problematic and costly. Accordingly, we envision that probe **1** and analogous fluorogenic affinity labels will be a useful addition to the armamentarium for the labeling of proteins *in cellulo*.

Experimental

Synthesis of 1

General—Amine **11** was a generous gift from the Promega Corporation (Madison, WI). Dimethylformamide (DMF), tetrahydrofuran (THF), and dichloromethane (CH_2Cl_2) were drawn from a Baker CYCLE-TAINER solvent delivery system. All other reagents were obtained from Sigma (Saint Louis, MO) or Fisher Scientific (Hanover Park, IL) and used without further purification.

Thin-layer chromatography was performed with aluminum-backed plates coated with silica gel containing F_{254} phosphor and visualized by UV illumination or staining with I_2, ceric ammonium molybdate, or phosphomolybdic acid. Flash chromatography was performed by using open columns loaded with silica gel-60 (230–400 mesh), or on a FlashMaster Solo system (Argonaut, Redwood City, CA) with Isolute Flash Si II columns (International Sorbent Technology, Hengoed, Mid Glamorgan, UK). The term “concentrated under reduced pressure” refers to the removal of solvents and other volatile materials using a rotary evaporator at water-aspirator pressure (<20 mm Hg) while maintaining the water-bath temperature below 40 °C. The term “high vacuum” refers to vacuum achieved by a mechanical belt-drive oil pump.

NMR spectra were obtained with a Bruker DMX-400 Avance spectrometer at the National Magnetic Resonance Facility at Madison (NMRFAM). Mass spectrometry was performed with a Micromass LCT (electrospray ionization, ESI) mass spectrometer in the Mass Spectrometry Facility in the Department of Chemistry.

Synthesis of succinic acid monobenzyl ester (5)—Compound **5** was synthesized according to a published procedure.[20] The white crystalline material afforded in the published procedure was dissolved in a minimal amount of 1:1 hexanes/EtOAc and cooled to 4 °C. Crystallization was initiated by the dropwise addition of hexane (~20 drops). The mixture was stored overnight at −20 °C. The crystals were isolated by filtration, washed with cold hexane (4 °C), and dried in the air. Residual solvent was removed under high vacuum to yield

compound **5** as a white crystalline solid (3.44 g, 83%). ^{1}H NMR (400 MHz, DMSO-d_6) δ (ppm): 12.25 (s, 1H), 7.36 (m, 5H), 5.10 (s, 2H), 2.58 (m, 2H), 2.50 (m, 2H). ^{13}C NMR (400 MHz, DMSO-d_6) δ (ppm): 173.47, 172.10, 136.25, 128.45, 128.00, 127.84, 65.53, 28.78, 28.72. HRMS (ESI): $[M+Na]^+$ calculated, 231.0628; found, 231.0635.

Synthesis of t-Boc–rhodamine–urea 6—Succinic acid monobenzyl ester (**5**; 193 mg, 0.929 mmol) was dissolved in anhydrous THF (2.0 mL) under Ar(g). Hünig's base (DIEA; 202 μL, 1.16 mmol) was then added, followed by the dropwise addition of diphenyl phosphoryl azide (DPPA; 256 mg, 0.929 mmol). The solution was stirred for 6 h and subsequently heated at reflux for an additional 2 h. Then, known *t*-Boc–rhodamine **4**[12] (100 mg, 0.232 mmol) was added, and the reaction mixture was stirred at reflux for 18 h. The reaction mixture was then partitioned between 5% v/v HCl(aq) and CH_2Cl_2. The organic extract was washed consecutively with 5% v/v HCl, water (3×), 5% w/v $NaHCO_3$(aq) (2×), water (3×), and saturated brine, and dried over $MgSO_4$(s). The solution was concentrated under reduced pressure, and the residue was purified by column chromatography (silica gel; first column: 5:3:2 hexanes/EtOAc/CH_2Cl_2→4:4:2 hexanes/EtOAc/CH_2Cl_2, second column: 0→2% v/v MeOH in CH_2Cl_2 containing AcOH (1% v/v), third column: 5:3:2 hexanes/EtOAc/CH_2Cl_2). Compound **6** was obtained as a pale yellow solid (137.2 mg, 93%). ^{1}H NMR (400 MHz, $CDCl_3$) δ (ppm): 7.99 (d, *J* = 7.0 Hz, 1H), 7.65-7.56 (m, 3H), 7.37-7.29 (m, 6H), 7.10 (s, 1H), 7.06 (m, 3H), 6.99 (d, *J* = 8.4 Hz, 1H), 6.66 (d, *J* = 8.6 Hz, 1H), 6.55 (d, *J* = 8.7 Hz, 1H), 6.00 (t, *J* = 5.6 Hz, 1H), 5.11 (s, 2H), 3.53 (dd, *J* = 11.5, 5.7 Hz, 2H), 2.62 (t, *J* = 6.1 Hz, 2H), 1.52 (s, 9H). ^{13}C NMR (400 MHz, $CDCl_3$) δ (ppm): 172.42, 170.12, 155.20, 152.59, 151.98, 151.82, 142.15, 141.21, 135.67, 135.25, 129.82, 128.57, 128.28, 128.18, 126.32, 125.29, 124.34, 115.40, 114.41, 112.91, 112.17, 106.34, 106.15, 81.17, 66.47, 35.71, 34.76, 28.33. HRMS (ESI): $[M+H]^+$ calculated, 636.2341; found, 636.2341.

Synthesis of rhodamine–urea 7—*t*-Boc–rhodamine–urea **6** (54.0 mg, 0.0848 mmol) was dissolved in CH_2Cl_2 (2.0 mL). Trifluoroacetic acid (TFA, 400 μL) was added, and the reaction mixture was stirred at 0 °C for 2 h. The reaction mixture was then allowed to warm to ambient temperature and stirred for an additional 3 h. The solution was concentrated under reduced pressure, and residual TFA was removed by azeotropic distillation with toluene. The residue was then dissolved in a minimal amount of acetone and purified by column chromatography (silica gel, 5→10% v/v MeOH:CH_2Cl_2) to afford compound **7** as an orange crystalline solid (40 mg, 88%). ^{1}H NMR (400 MHz, acetone-d_6) δ (ppm): 8.34 (s, 1H), 7.97 (d, *J* = 7.6 Hz, 1H), 7.81-7.76 (m, 2H), 7.70 (t, *J* = 7.1 Hz, 1H), 7.39-7.25 (m, 6H), 6.92 (dd, *J* = 8.6, 2.2 Hz, 1H), 6.61 (d, *J* = 8.6 Hz, 1H), 6.58 (d, *J* = 2.1 Hz, 1H), 6.47 (d, *J* = 8.5 Hz, 1H), 6.42 (dd, *J* = 8.5, 2.1 Hz, 1H), 6.09 (br, 1H), 5.14 (m, 2H), 3.50 (q, *J* = 6.3 Hz, 2H), 2.63 (t, *J* = 6.5 Hz, 2H), 2.09 (s, 2H). HRMS (ESI): $[M+H]^+$ calculated, 536.1822; found, 536.1816.

Synthesis of trimethyl lock–rhodamine–urea 9—Compound **7** (39.0 mg, 0.0728 mmol) was dissolved in 2.0 mL DMF and 2.0 mL pyridine. Trimethyl lock acid **8**[21] (38.5 mg, 0.146 mmol) and 1-ethyl-3-(3-dimethylaminopropyl)carbodiimide (EDC; 28 mg, 0.146 mmol) were then added, and the reaction mixture was stirred overnight at ambient temperature. The solution was concentrated under reduced pressure, and the residue was dissolved in CH_2Cl_2 (200 mL). The resulting solution was washed consecutively with 5% v/v HCl(aq), water, saturated $NaHCO_3$(aq), and saturated brine. The organic fraction was dried over Na_2SO_4(s). The residue was purified by column chromatography (silica gel, 4:6→5:5 hexanes/EtOAc) to give compound **9** as an orange solid (46 mg, 81%). ^{1}H NMR (400 MHz, $CDCl_3$) δ (ppm): 7.98 (d, *J* = 7.3 Hz, 1H), 7.66-7.56 (m, 3H), 7.38 (s, 1H), 7.32 (s, 5H), 7.20 (s, 1H), 7.06-7.02 (m, 3H), 6.80 (s, 1H), 6.67-6.61 (m, 2H), 6.57-6.53 (m, 2H), 5.74 (t, *J* = 5.7 Hz, 1H), 5.12 (s, 2H), 3.57-3.50 (m, 2H), 2.63-2.61 (m, 4H), 2.43 (s, 3H), 2.37 (s, 3H), 2.21 (s, 3H), 1.69-1.67 (m, 6H). ^{13}C NMR (400 MHz, $CDCl_3$) δ (ppm): 172.40, 171.96, 170.39, 170.24, 155.18, 153.15,

151.48, 149.97, 141.74, 139.91, 138.85, 137.18, 135.70, 135.31, 133.13, 132.96, 129.75, 128.55, 128.25, 128.13, 126.18, 124.90, 124.10, 123.42, 115.32, 114.93, 113.70, 111.65, 107.66, 106.22, 83.74, 66.38, 50.81, 40.25, 35.60, 34.77, 32.02, 25.53, 21.93, 20.16. HRMS (ESI): $[M+H]^+$ calculated, 782.3073; found, 782.3062.

Synthesis of trimethyl lock–rhodamine–urea 10—Ethanol (10 mL) was added to compound **9** (35 mg, 0.045 mmol) and Pd/C (10% w/w, 14 mg) at −5 °C. The resulting mixture was stirred under an H_2(g) atmosphere for 30 min. The reaction mixture was filtered through celite and washed consecutively with CH_2Cl_2 and EtOH. The washings were combined and concentrated under reduced pressure. The residue was then adsorbed onto celite and purified by column chromatography (silica gel, 0→10% v/v MeOH in CH_2Cl_2 containing 1% v/v AcOH) to afford compound **10** as a pale-yellow solid (26 mg, 84%). ^{1}H NMR (400 MHz, $CDCl_3$) δ (ppm): 8.00-7.90 (m, 2H), 7.84 (s, 1H), 7.59-7.49 (m, 2H), 7.34 (s, 1H), 7.22 (s, 1H), 6.95 (d, *J* = 7.3 Hz, 1H), 6.81 (d, *J* = 7.2 Hz, 1H), 6.74 (s, 1H), 6.64-6.55 (m, 2H), 6.53-6.42 (m, 2H), 6.10 (b, 1H), 3.39 (s, 2H), 2.62 (s, 2H), 2.46 (s, 2H), 2.39 (s, 3H), 2.32 (s, 3H), 2.16 (s, 3H), 1.63 (s, 6H). ^{13}C NMR (400 MHz, $CDCl_3$) δ (ppm): 176.38, 171.97, 170.60, 170.04, 155.88, 152.83, 151.52, 151.48, 149.89, 141.58, 139.74, 138.76, 137.08, 135.31, 133.03, 132.93, 129.77, 128.00, 126.17, 124.87, 124.03, 123.35, 115.45, 114.93, 113.94, 111.88, 107.83, 106.40, 83.66, 50.65, 40.17, 35.53, 34.76, 32.00, 25.48, 21.88, 20.12. HRMS (ESI): $[M+Na]^+$ calculated, 714.2422; found, 714.2396.

Synthesis of probe 1—Compound **10** (26 mg, 0.038 mmol) was dissolved in DMF (1.0 mL) and pyridine (1.0 mL each). EDC (22 mg, 0.113 mmol) was added, and the resulting mixture was stirred for 1 h. *N*-Hydroxysuccinimide (NHS; 13 mg, 0.113 mmol) was then added, and the reaction mixture was stirred for 36 h under Ar(g). The solution was concentrated under reduced pressure, and the residue was partitioned between 10% w/v citric acid(aq) and CH_2Cl_2. The layers were separated, and the aqueous layer was extracted with CH_2Cl_2. The organic extracts were combined, washed consecutively with water and saturated brine, and dried over Na_2SO_4(s) to give the crude succinimide intermediate as a pale-yellow solid (35 mg). This intermediate (35 mg) was then dissolved in 2.0 mL of 9:1 DMF/DIEA. Amine **11** (10 mg, 0.044) was added, and the reaction mixture was stirred under Ar(g) for 72 h. The solution was concentrated under reduced pressure, and the residue was partitioned between EtOAc and 6% v/v HCl(aq). The layers were separated, and the aqueous phase was extracted with EtOAc. The organic extracts were combined, washed consecutively with water and saturated brine, and dried over Na_2SO_4(s). Probe **1** was isolated by column chromatography (silica gel; first column: 5:3:2 hexanes/EtOAc/CH_2Cl_2, second column: 2% v/v MeOH in CH_2Cl_2) as an off-white solid (12.5 mg, 32%). ^{1}H NMR (400 MHz, $CDCl_3$) δ (ppm): 7.98 (d, *J* = 6.5 Hz, 1H), 7.87 (s, 1H), 7.60 (dt, *J* = 4.3, 1.4 Hz, 2H), 7.46 (s, 1H), 7.39 (dd, *J* = 10.3, 2.2 Hz, 2H), 7.09 (d, *J* = 7.3 Hz, 1H), 6.97 (dd, *J* = 8.6, 2.2 Hz, 1H), 6.79 (s, 1H), 6.62-6.52 (m, 4H), 6.17 (br, 1H), 5.80 (br, 1H), 3.62 (s, 4H), 3.53-3.45 (m, 10H), 2.56 (m, 2H), 2.42 (m, 5H), 2.38 (s, 3H), 2.23 (s, 3H), 1.75-1.64 (m, 8H), 1.63-1.54 (m, 2H), 1.46-1.26 (m, 4H). HRMS (ESI): $[M+Na]^+$ calculated, 919.3656; found, 919.3617.

Cell imaging

General—Probe **2** and U2OS cells were generous gifts from Promega. Probe **3** was from Promega. Rhodamine 110 was from Sigma–Aldrich. Cell-culture medium was from Invitrogen or Hyclone (Fisher Scientific). Dulbecco's phosphate-buffered saline (PBS) and fetal bovine serum were from Invitrogen. Porcine liver esterase, MW ~163 kDa, as a suspension in 3.2 M $(NH_4)_2SO_4$ was from Sigma Chemical (product number E2884). For labeling experiments, fluorogenic and fluorescent probes were stored as stock concentrations in DMSO and diluted such that DMSO concentration did not exceed 1%. Absorbance measurements were recorded

at ambient temperature (23 ± 2 °C) in 1-cm path-length cuvettes on a Cary model 50 spectrometer from Varian.

Cell Preparation—U2OS cells (ATCC HTB-96TM) were plated on glass-bottom culture dishes (35 × 10 mm; Electron Microscopy Sciences) and grown to 60–90% confluence at 37 °C in McCoy's 5A modified media containing FBS (10% v/v). Prior to the addition of probes, the medium was replaced with phenol red-free McCoy's 5A medium (800 μL) that had been incubated at 37 °C. Probes were dissolved at a 5× working concentration in phenol red-free medium (200 μL) that had been incubated at 37 °C. For the experiments with unmasked probes (Figure 2D), porcine liver esterase (10 μL, 1.66 U/μL) was then added, and the resulting medium was incubated at room temperature for 3½ h. The probe-containing medium was added to the cell-containing medium, and the resulting medium was incubated at 37 °C. Cells were visualized by confocal microscopy after 10, 15, or 30 min.

Microscopy—Images of cells were obtained with a Nikon Eclipse TE2000-U confocal microscope equipped with a Zeiss AxioCam digital camera. Excitation at 488 nm was provided by an argon-ion laser, and emission light was passed through a filter centered at 515 nm and having a 40-nm band-pass. Brightfield images indicated that the cells were alive and appeared to have normal physiology, both before and after imaging.

Ultraviolet–visible spectroscopy

For each measurement, a probe was initially added to 20 μL PBS. To unmask the fluorescence of **1**, porcine liver esterase (3.0 μL, 1.66 U/μL) was added, and the solution was left at ambient temperature for 4 h. Then, varying ratios of water and dioxane were added to a final volume of 200 μL, and absorbance was measured from 400–600 nm.

Calculation of log*D*

The parameter log*D* refers to the ratio of concentration of all probe microspecies (including both ionized and neutral forms) in octanol to that in water, according to eq 1:[24,25]

$$\log D = \log\left(\frac{\sum[\text{microspecies}]_{\text{octanol}}}{\sum[\text{microspecies}]_{\text{water}}}\right) \quad (1)$$

Values of log*D* were calculated with ACD/PhysChem Suite, version 12.[29] Parameters of fluorescein (pK_a 6.32[30]; log*D* −0.9931) and rhodamine 110 (log*D* 0.832) were entered into the software training database.

Supplementary Material

Refer to Web version on PubMed Central for supplementary material.

Acknowledgments

We are grateful to the Promega Corporation for gifts of compounds **2** and **11**, and U2OS cells. This work was supported by grant CA073808 (NIH). R.W.W. was supported by an NSF Graduate Research Fellowship and by Chemistry–Biology Interface Training Grant GM008505 (NIH). L.D.L was supported by an ACS Division of Organic Chemistry Fellowship sponsored by the Genentech Foundation and by Biotechnology Training Grant GM008349 (NIH). V.M.K. was supported by a Barry M. Goldwater Scholarship and a Hilldale Undergraduate/Faculty Research Fellowship. NMRFAM was supported by grant P41RR02301 (NIH).

References

1. Teodori L, Bushnell T, Campanella L, Tárnok A. Cytometry 2008;73A:1109–1110. [PubMed: 18985727]
2. Chalfie, M.; Kain, SR., editors. Green Fluorescent Protein: Properties, Applications, and Protocols. Vol. 2nd ed.. Hoboken, NJ: John Wiley & Sons; 2006.
3. Lavis LD, Raines RT. ACS Chem. Biol 2008;3:142–155. [PubMed: 18355003]
4. Los GV, Encell LP, McDougall MG, Hartzell DD, Karassina N, Zimprich C, Wood MG, Learish R, Ohana RF, Urh M, Simpson D, Mendez J, Zimmerman K, Otto P, Vidugiris G, Zhu J, Darzins A, Klaubert DH, Bulleit RF, Wood KV. ACS Chem. Biol 2008;3:373–382. [PubMed: 18533659]
5. Agard NJ, Baskin JM, Prescher JA, Lo A, Bertozzi CR. ACS Chem. Biol 2006;1:644–648. [PubMed: 17175580]
6. Soellner MB, Nilsson BL, Raines RT. J. Am. Chem. Soc 2006;128:8820–8828. [PubMed: 16819875]
7. Ning X, Guo J, Wolfert MA, Boons G-J. Angew. Chem. Int. Ed 2008;47:2253–2255.
8. Los GV, Wood K. Methods Mol. Biol 2007;356:195–208. [PubMed: 16988404]
9. Milstein S, Cohen LA. J. Am. Chem. Soc 1972;94:9158–9165. [PubMed: 4642365]
10. Borchardt RT, Cohen LA. J. Am. Chem. Soc 1972;94:9166–9174. [PubMed: 4642366]
11. Chandran SS, Dickson KA, Raines RT. J. Am. Chem. Soc 2005;127:1652–1653. [PubMed: 15700995]
12. Lavis LD, Chao T-Y, Raines RT. ACS Chem. Biol 2006;1:252–260. [PubMed: 17163679]
13. Huang ST, Lin YL. Org. Lett 2006;8:265–268. [PubMed: 16408891]
14. Lavis LD, Chao T-Y, Raines RT. ChemBioChem 2006;7:1151–1154. [PubMed: 16755624]
15. Johnson RJ, Chao T-Y, Lavis LD, Raines RT. Biochemistry 2007;46:10308–10316. [PubMed: 17705507]
16. Levine MN, Lavis LD, Raines RT. Molecules 2008;13:204–211. [PubMed: 18305412]
17. Mangold SL, Carpenter RT, Kiessling LL. Org. Lett 2008;10:2997–3000. [PubMed: 18563907]
18. Yatzeck MM, Lavis LD, Chao TY, Chandran SS, Raines RT. Bioorg. Med. Chem. Lett 2008;18:5864–5866. [PubMed: 18595692]
19. Turcotte RF, Lavis LD, Raines RT. FEBS J 2009;276:4270–4281.
20. Winkler J, Urban E, Losert D, Wacheck V, Pehamberger H, Noe CR. Nucleic Acids Res 2004;32:710–718. [PubMed: 14757835]
21. Amsberry KL, Borchardt RT. J. Org. Chem 1990;55:5867–5877.
22. Zaikova TO, Rukavishnikov AV, Birrell GB, Griffith OH, Keana JFW. Bioconjug. Chem 2001;12:307–313. [PubMed: 11312693]
23. Monnè L. Proc. Soc. Exp. Biol. Med 1935;32:1197–1199.
24. van de Waterbeemd H, Testa B. Adv. Drug Res 1987;16:85–225.
25. van de Waterbeemd, H. Drug Bioavailability: Estimation of Solubility, Permeability, Absorption, and Bioavailability. Vol. 2nd ed.. van de Waterbeemd, H.; Lennernas, H.; Arturrson, P., editors. Weinheim, Germany: Wiley–VHC; 2009. p. 71-100.
26. Camenisch G, Alsenz J, van de Waterbeemd H, Folkers G. Eur. J. Pharm. Sci 1998;6:313–319.
27. Ioffe IS, Otten VF. Zh. Obshch. Khim 1965;1:333–336.
28. Kuila K SC, Lahiri. Z. Phys. Chem 2004;218:803–828.
29. [Accessed: 29 April 2009]. www.acdlabs.com/physchemsuite
30. Goldberg JM, Baldwin RL. Biochemistry 1998;37:2546–2555. [PubMed: 9485404]
31. Cheruvu NP, Kompella UB. Invest. Ophthalmol. Vis. Sci 2006;49:333–341. [PubMed: 18172110]
32. Lampidis TJ, Castello C, del Giglio A, Pressman BC, Viallet P, Trevorrow KW, Valet GK, Tapiero H, Savaraj N. Biochem. Pharmacol 1989;38 4267-2471.

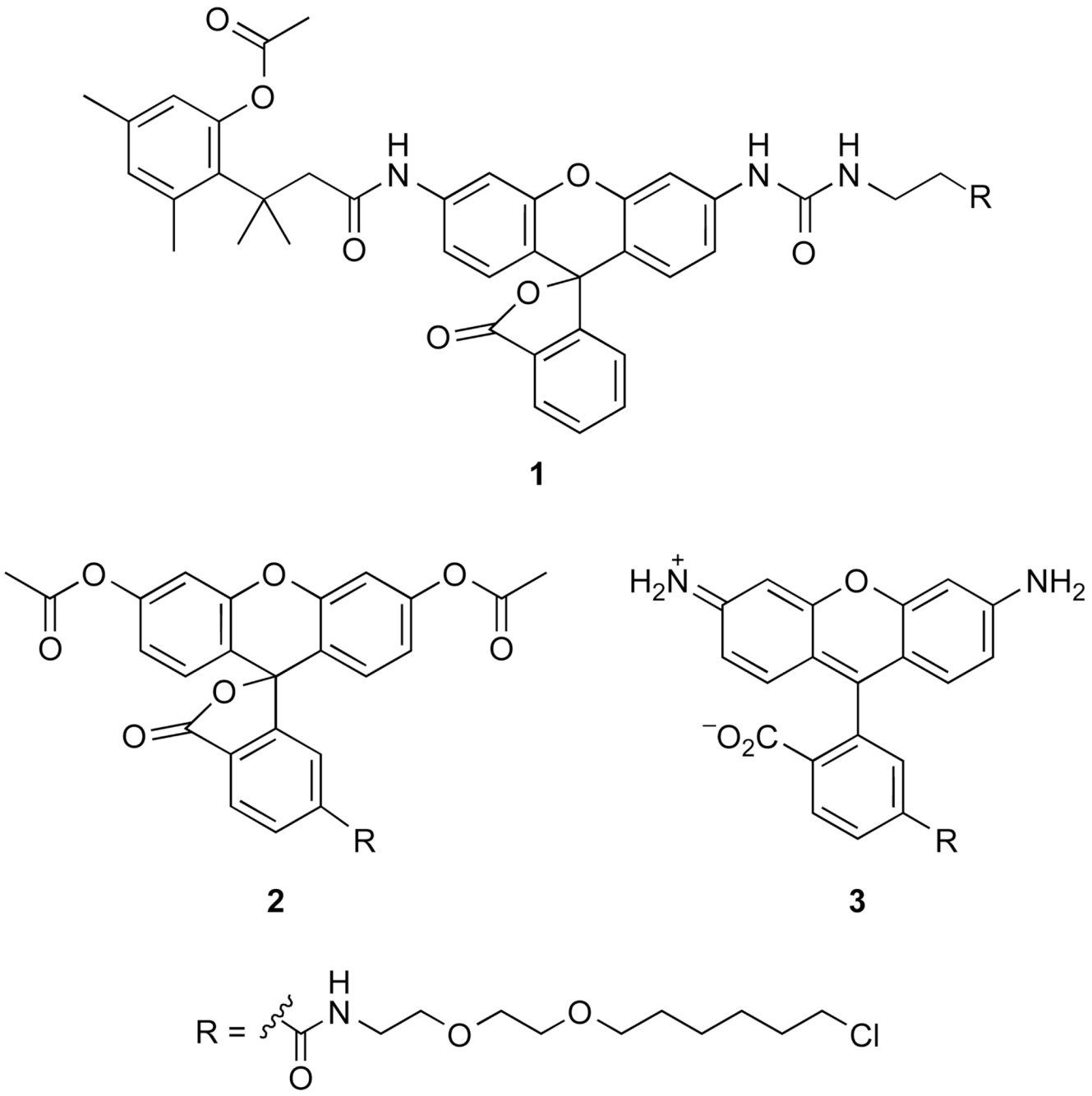

Figure 1.
Fluorogenic (**1** and **2**) and fluorescent (**3**) labels for haloalkane dehalogenase.

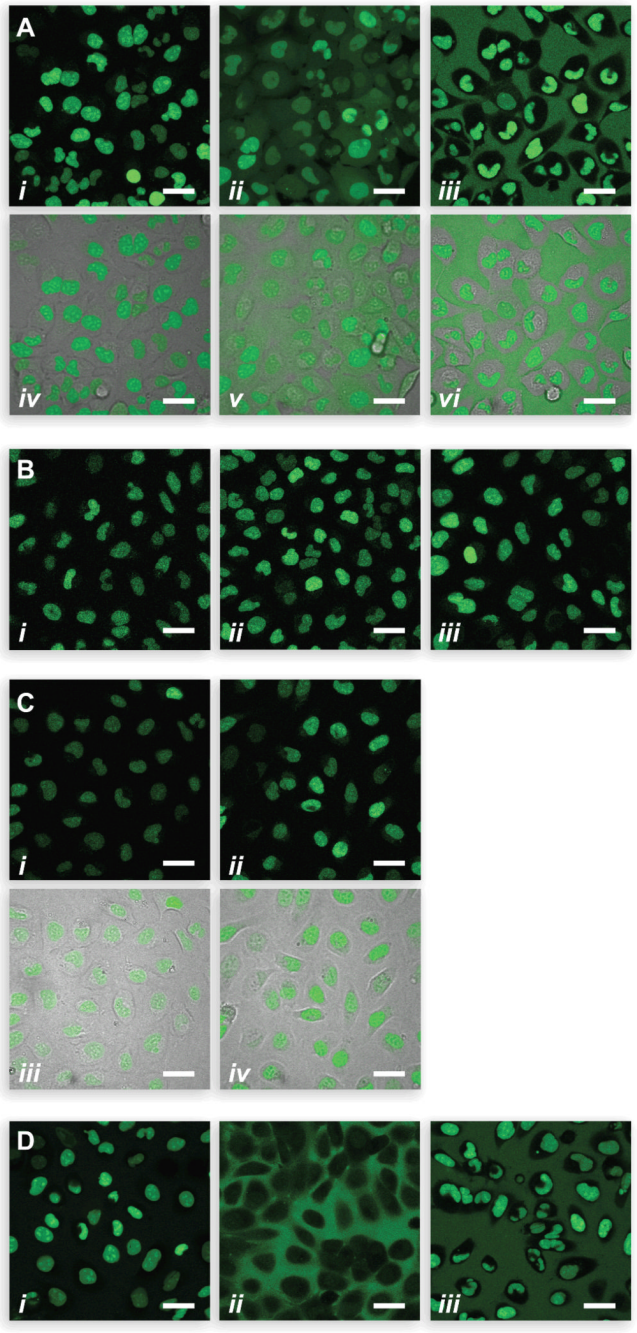

Figure 2.

Labeling of an HD variant (HaloTag®–NLS_3) in live, unwashed U2OS cells at 37 °C as visualized by confocal microscopy. Scale bars = 200 μm. (A) Effect of probe type. Probe (1.0 μM) was incubated with cells for 15 min; (*i*) **1**, (*ii*) **2**, (*iii*) **3**, (*iv*, *v*, and *vi*) overlay with brightfield images. (B) Effect of incubation time. Probe **1** (1.0 μM) was incubated with cells for (*i*) 10 min, (*ii*) 15 min, and (*iii*) 30 min. (C) Effect of probe concentration. Probe **1** was incubated with cells for 15 min at (*i*) 1 μM, (*ii*) 10 μM, (*iii* and *iv*) overlay with brightfield images. (D) Effect of probe unmasking. Probe (1.0 μM) was incubated with cells for 15 min; (*i*) unmasked **1**, (*ii*) unmasked **2**, and (*iii*) **3**.

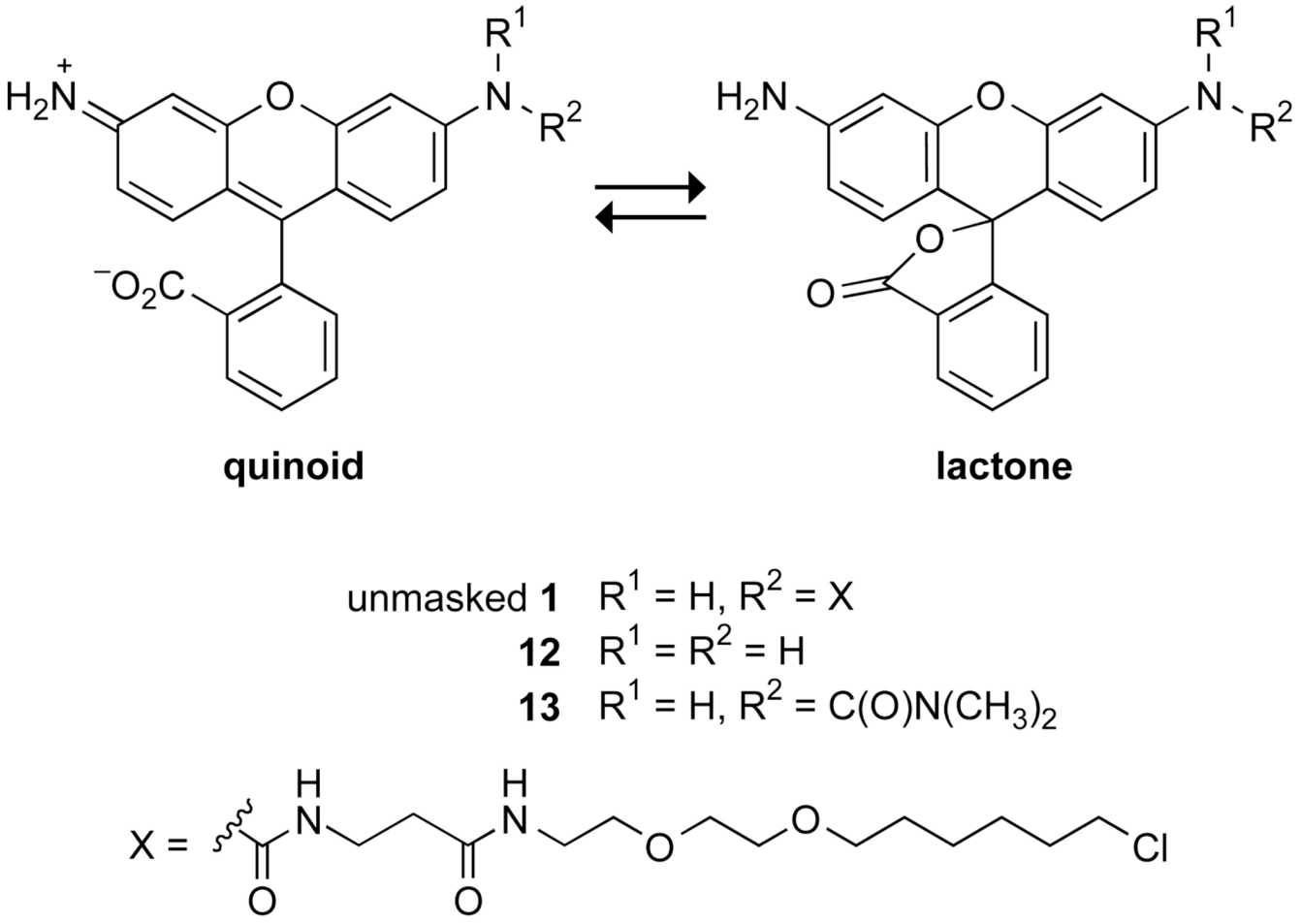

Figure 3.
Lactone–quinoid equilibrium of **1**, **12**, and **13**.

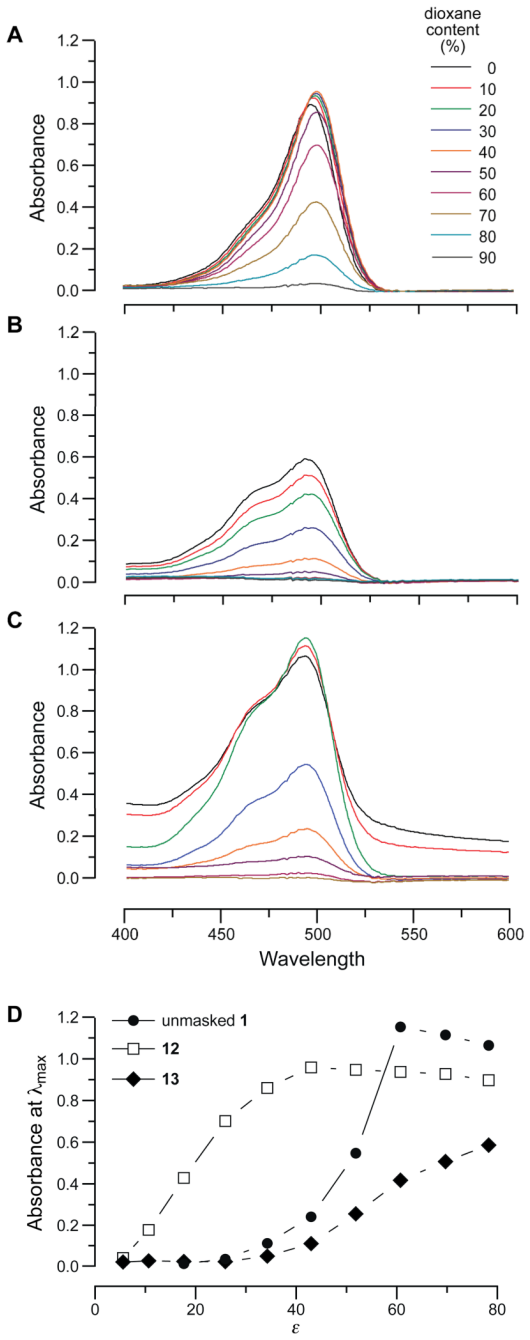

Figure 4.

Effect of dielectric constant on the lactone–quinoid equilibrium of unmasked **1**, **12**, and **13**. Absorption spectra of (A) unmasked 1 (50 μM), (B) **12** (12.5 μM), and (C) **13** (12.5 μM) in mixtures of dioxane and water. (D) Absorption at λ_{max} in the spectra in panels A–C. Values of ε are from ref. [28].

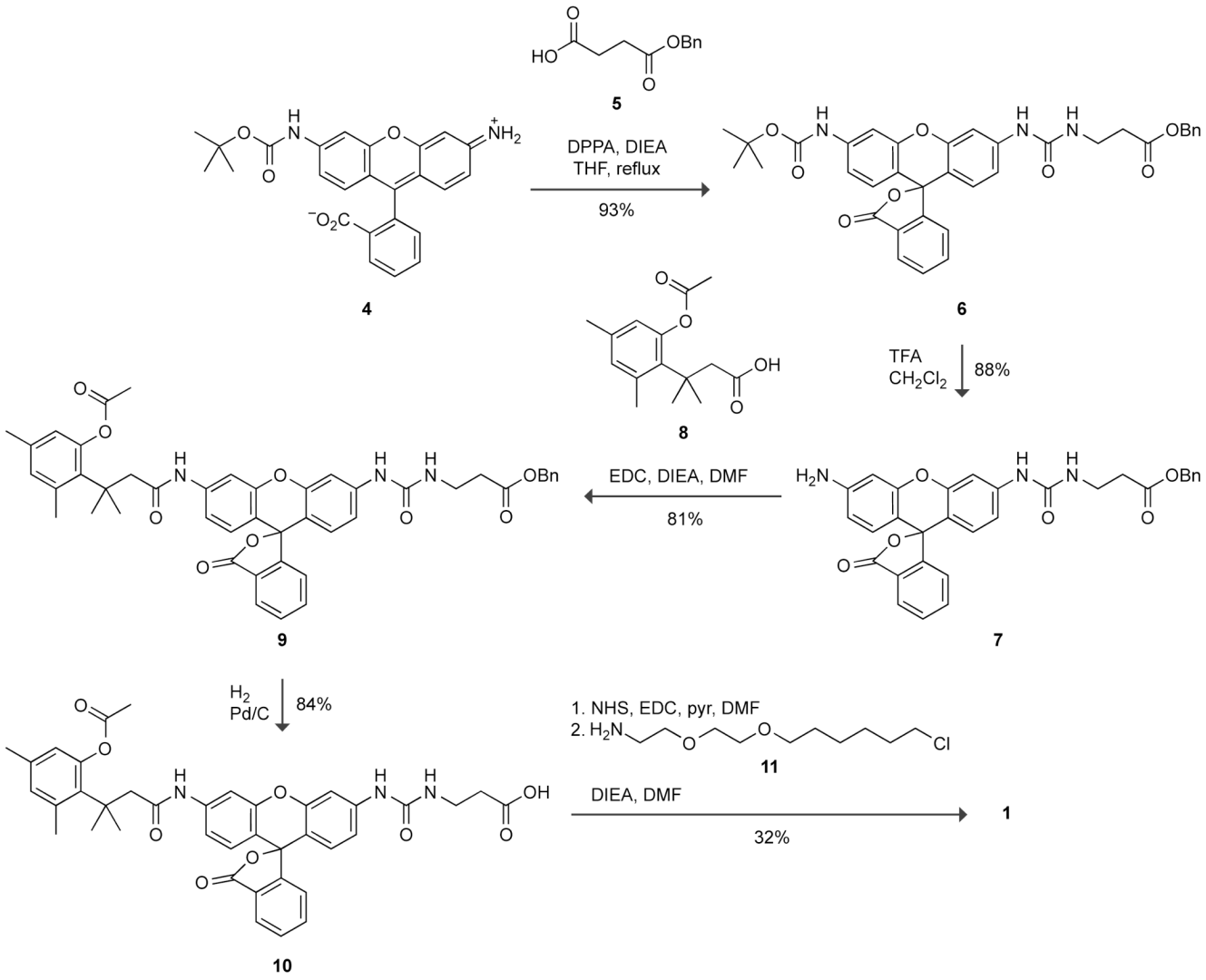

Scheme 1.
Synthesis of probe **1**.

Table 1

Calculated values of log*D* for masked and unmasked probes at pH 7.4.

Probe	log*D*
1	4.82
2	3.93
3	2.37
	2.63

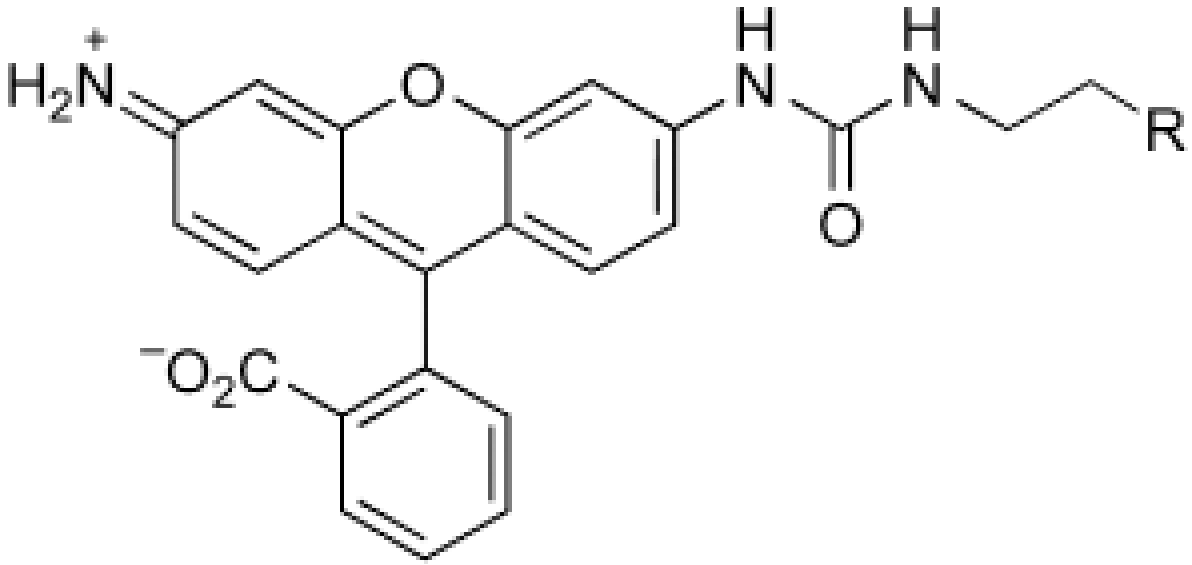

Probe	log*D*
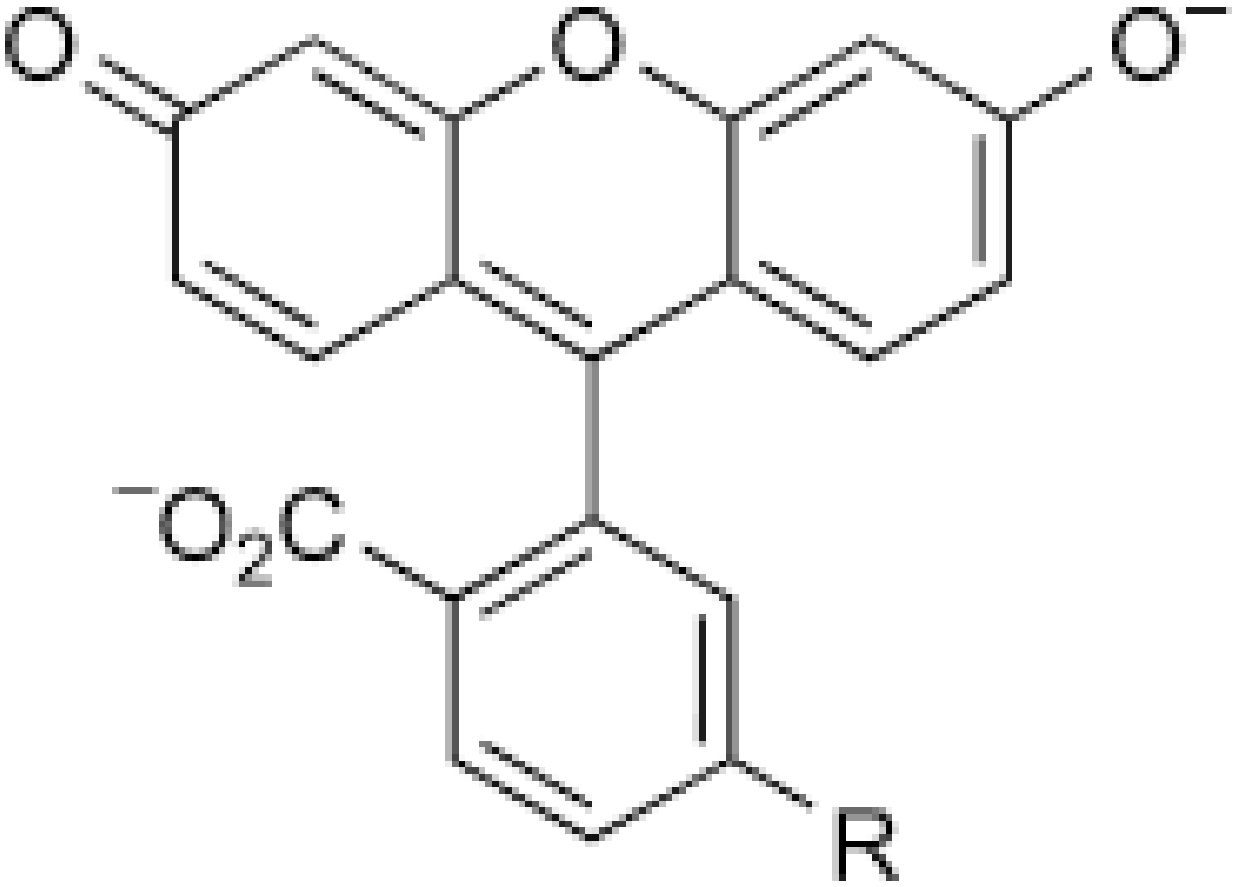	0.12